

Computed tomography—current status and future directions for arthritis imaging

Sevtap Tugce Ulas  and Torsten Diekhoff*Ther Adv Musculoskelet Dis*

2024, Vol. 16: 1–13

DOI: 10.1177/
1759720X241287373© The Author(s), 2024.
Article reuse guidelines:
sagepub.com/journals-
permissions

Abstract: Applications of computed tomography (CT) in arthritis imaging have rapidly expanded in recent years due to ongoing technical developments. Dual-energy CT (DECT) has become indispensable in clinical practice, particularly for diagnosing gouty arthritis and assessing bony structural changes. Technological innovations such as low-dose CT and state-of-the-art reconstruction algorithms reduce radiation exposure while maintaining image quality and short acquisition times. This review explores the growing role of CT in arthritis imaging. Recent innovations have extended DECT's utility beyond gout diagnosis to the detection of inflammatory changes in various arthritic conditions. Postprocessing techniques such as the generation of subtraction images and iodine maps provide valuable insights into tissue perfusion and inflammatory activity, crucial for arthritis management. DECT can distinguish calcium from uric acid crystals, facilitating the differential diagnosis of various crystal arthropathies in a variety of clinical settings. This ability is particularly valuable in distinguishing between different clinical conditions in patients with inflammatory joint changes within a single imaging examination. Moreover, the advent of four-dimensional CT promises a better assessment of dynamic joint instabilities and ligament injuries, especially in the wrist. Overall, DECT offers a comprehensive approach to arthritis imaging, from the detection of structural changes to the assessment of active inflammation in joints and tendons. Continuous advances in CT technology, including photon-counting CT, hold promise for further improving diagnostic accuracy and expanding the role of CT in arthritis imaging and therapy monitoring.

Keywords: arthritis imaging, computed tomography, dual-energy CT

Received: 11 February 2024; revised manuscript accepted: 11 September 2024.

Introduction

While computed tomography (CT) of the peripheral skeleton was for a long time reserved for imaging trauma, dual-energy computed tomography (DECT) has gained increasing importance in recent years and has already become established for diagnostic assessment in several other conditions in clinical routine.¹ This is particularly true for gout, as DECT reliably detects monosodium urate (MSU) crystals,² distinguishes them from other crystal species, and can quantify their volume or mass.^{3,4} Furthermore, DECT's role in the diagnostic process is fully recognized by the 2015 ACR/EULAR classification criteria,⁵ the 2018 EULAR imaging recommendation for gout,⁶ and the 2023 EULAR imaging recommendation for crystal arthropathies.⁷ With its high spatial

resolution and direct depiction of bone, CT is considered the reference standard for evaluating bony structural changes, such as erosions. CT thus allows more accurate serial monitoring of joint damage, as may occur when patients with rheumatic diseases are not treated adequately, compared with the current standard of ultrasound and X-ray.^{8,9}

In contrast to conventional CT, DECT captures the attenuation of high- and low-energy X-ray photons separately. Photon attenuation in biological tissues is influenced by the Compton effect and the photoelectric effect, which, in turn, depend on tissue material properties (i.e., the effective atomic number) and X-ray beam energy, respectively.¹⁰ Moreover, various reconstruction

Correspondence to:

Sevtap Tugce Ulas
Department of
Radiology, Charité—
Universitätsmedizin
Berlin, Campus Mitte,
Humboldt—Universität zu
Berlin, Freie Universität
Berlin, Charitéplatz 1,
Berlin 10117, Germany
Berlin Institute of
Health at Charité—
Universitätsmedizin
Berlin, Berlin, Germany
sevtap-tugce.ulas@charite.de

Torsten Diekhoff
Department of
Radiology, Charité—
Universitätsmedizin
Berlin, Campus Mitte,
Humboldt—Universität zu
Berlin, Freie Universität
Berlin, Berlin, Germany
Berlin Institute of
Health at Charité—
Universitätsmedizin
Berlin, Berlin, Germany

methods can be applied to extract additional information on morphological changes from DECT scans.¹¹

Until recently, DECT did not play a significant role in arthritis imaging outside the context of gout because of limitations in the detection of inflammatory joint changes.^{12,13} However, the applications of DECT in arthritis imaging have significantly increased in recent years, not solely due to ongoing technical development. Initial studies demonstrate promising results in detecting active inflammation.^{14,15} Various reconstruction methods are of particular interest, including subtraction techniques¹⁶ and specific iodine maps.^{15,17} With these methods, it is possible to measure contrast agent uptake in the synovium of joints or tendon sheaths, providing information on tissue perfusion and inflammatory activity.¹⁸

Another advantage of DECT in musculoskeletal imaging is the option of enhancing image quality by subtracting metal artifacts, which can be caused by implants or osteosynthesis materials.¹⁹ In ultrasound and magnetic resonance imaging (MRI) examinations, metal artifacts often lead to considerable uncertainties in the assessment of subtle changes, especially in early arthritis. An essential concern in the use of CT imaging is radiation exposure. However, state-of-the-art CT protocols and reconstruction algorithms, such as low-dose CT techniques and reconstruction with iterative or artificial intelligence algorithms, significantly reduce radiation exposure to levels similar to those of conventional radiography.²⁰ Iterative reconstruction improves image quality compared with the former standard filtered back projection.²¹ One of the advantages of CT imaging is its rapid availability and short acquisition time. Similar to a conventional X-ray examination, a CT scan including positioning takes about 5 min, compared to approximately 30 min for an MRI and around 15 min for an ultrasound examination, depending on the sonographer's experience.¹⁶

All technical advances outlined above have considerably expanded the role of CT imaging in clinical practice beyond its sole use in gout. This review aims to provide an overview of the range of applications of CT in arthritis imaging today.

Detection of structural changes

In addition to inflammatory changes, reliable demonstration of structural lesions in peripheral

joints is crucial for the differential diagnosis and of particular significance in the clinical setting. DECT imaging offers a crucial advantage in the detection of such structural changes, not least due to its superior spatial resolution.

Erosion

Erosions are among the hallmarks of the different forms of arthritic conditions.²² They typically occur after a prolonged episode of disease activity or in patients with inadequate therapy.²³ The development of erosions is often accompanied by progressive joint dysfunction. Accordingly, their detection and monitoring over time by imaging plays a crucial role in clinical practice. For this reason, a highly standardizable imaging technique is necessary to differentiate these changes reliably and as early as possible.

In clinical practice, X-ray has established itself as the initial imaging modality for patients presenting with arthritis.⁹ However, X-ray has a notoriously low sensitivity for joint erosion compared with cross-sectional imaging techniques.⁹ While ultrasound can provide a more sensitive depiction of these lesions compared to X-ray, there is a risk of overestimating imaging findings for nonspecific structures, such as bone canals. Similar limitations have been reported for erosion detection by MRI.^{24,25} Initial studies have investigated optimized sequence techniques with CT-like images using susceptibility-weighted sequences^{26,27} or ultra-short echo time²⁸ and zero echo time,²⁹ incorporating artificial intelligence algorithms.³⁰ While these techniques show promise for future improvement of MRI protocols, they have not yet been widely investigated and established in clinical routine and merely try imitating the original CT scan. With its high spatial resolution and the ability to directly depict the cortical bone, CT detects these changes more accurately than ultrasound, X-ray, and MRI. CT has thus emerged as the reference standard in erosion detection.

Detection of dynamic wrist instabilities using four-dimensional CT

The future of CT imaging promises significant progress through innovative technologies such as four-dimensional CT (4D-CT).³¹ 4D-CT opens new dimensions for imaging by enabling excellent assessment of both static and dynamic phenomena of three-dimensional structures within complex anatomy,^{32,33} see also Figure 1. The latest

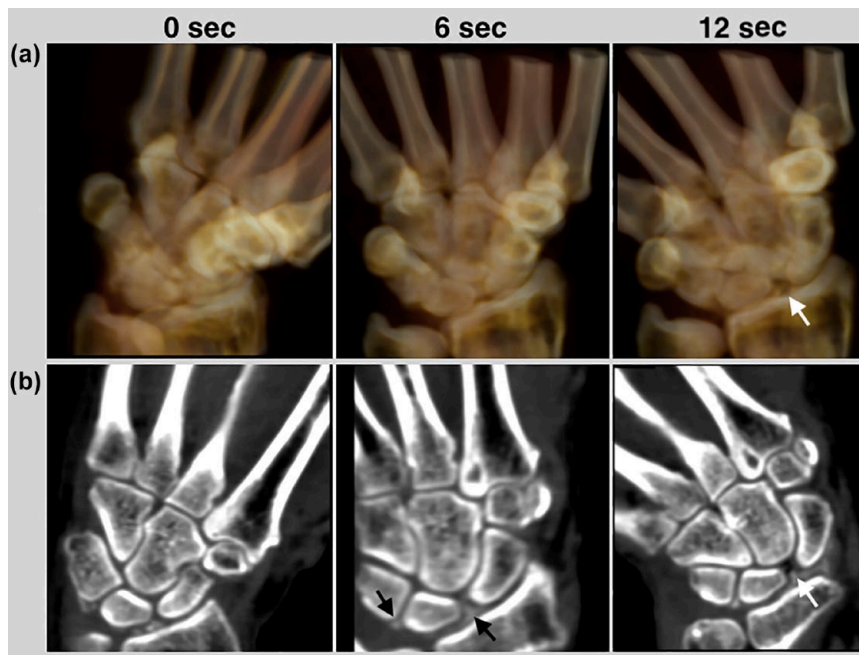


Figure 1. 4D-CT of the wrist in a patient with CPPD disease. (a) Dynamic 3D reconstruction. (b) Dynamic 2D reconstruction. In ulnar abduction, a clear dissociation of the SL joint space as a correlate of SL ligament rupture (white arrow) is seen. In addition, ligament calcifications characteristic of CPPD are apparent in the wrist (black arrows).

CPPD, calcium pyrophosphate deposition; 4D-CT, Four-dimensional computed tomography; SL, scapholunate.

CT detectors allow the acquisition of images during motion,³² which provide deeper insights into pathobiomechanical joint changes.³⁴ Use of 4D-CT in the detection of scapholunate interosseous ligament injuries demonstrates its potential utility in diagnosing wrist injuries. In the context of peripheral joint imaging, 4D-CT allows differentiated detection of static and dynamic joint instabilities, which can lead to accelerated degenerative changes over time.³⁵ This is particularly important in calcium pyrophosphate deposition (CPPD) arthropathy, where crystal deposits in the wrist can lead to changes in ligamentous structures and wrist biomechanics, causing wrist instabilities.^{35,36} The carpal region is a key focus for 4D-CT imaging due to the limitations of traditional techniques in accurately capturing certain motion patterns, particularly in patients with distal radioulnar joint instability.

Crystal arthropathies—the potential of two-material decomposition

A crucial strength of DECT over conventional CT is its ability to differentiate between two different substances based on their distinct attenuation coefficients. This involves comparing the

attenuation coefficients of individual voxels within a defined density range. For instance, it enables the assignment of values for calcium (~ 0.69) or MSU (~ 1.07).³⁷ This additional information is helpful for a wide range of applications in clinical routine, especially the differential diagnosis of inflammatory joint changes in a single imaging examination.

Calcium pyrophosphate deposition. CPPD arthropathy is characterized by the accumulation of crystals in the ligaments of the wrist, resulting in inflammation and ligament damage mediated by interleukin-1 β .³⁸ With its acute inflammatory (pseudogout) and chronic inflammatory (pseudo-RA) subtypes, CPPD is another differential diagnosis of rheumatoid arthritis (RA), particularly in older patients. The underlying cause is disturbed calcium metabolism with increased calcium deposition, especially in peripheral ligaments and joints. These crystalline calcium pyrophosphate (CPP) deposits can rapidly progress to irreversible cartilage destruction, significantly limiting joint function. With its high spatial resolution, DECT can reliably detect these calcifications and determine crystal species through two-material differentiation.^{39,40} For this reason, DECT also

holds an important role in the diagnostic process for CPPD, in accordance with the current ACR/EULAR criteria.⁴¹ Such ligament calcifications can be subtle and may elude detection by X-ray or arthrosonography when present in anatomical structures that are less amenable to the X-ray beam or the ultrasound probe such as the palmar carpal ligaments. MRI often misses these changes as hypointense crystals show low contrast to hypointense ligaments, even in images acquired with special gradient-echo sequences. Initial clinical studies have additionally demonstrated that CPPD exhibits specific DECT attenuation properties, which can be utilized for more precise assessment and characterization of meniscal calcifications.^{42,43} Although DECT holds promise in the characterization of intra-articular mineralization within the knee joint,⁴⁴ this modality currently lacks the precision to reliably detect early calcium crystal accumulation that does not manifest as chondrocalcinosis on standard CT imaging.⁴⁵ Furthermore, DECT does not sufficiently allow to effectively discriminate between CPP and basic calcium phosphate crystals.⁴⁶

Gout. Gout goes along with MSU crystal depositions in the body specifically in peripheral joints and is an important differential diagnosis in patients with peripheral joint diseases.⁵ DECT allows solid differentiation between MSU and calcium through its two-material differentiation capability.⁴⁷ This way, gouty tophi can be visualized and quantitatively measured without the need for contrast agent administration.⁴⁸ Furthermore, DECT also allows for a quantitative assessment of treatment response, enabling continuous monitoring of MSU crystals.⁴⁹ In addition to detecting these MSU crystals, DECT also visualizes typical bone changes in gout.⁴ First studies suggest that DECT may have the capability to identify MSU crystal deposits in vascular structures,^{50,51} while there are also concerns regarding the specificity in the detection of these plaques.⁵²

Collagen mapping

Collagen is the primary constituent of tendons and ligaments, which play a critical role in load distribution and force transmission. DECT enables not only the visualization of MSU crystal deposition but also the generation of collagen maps based on its specific capability of three-material differentiation. This technique assumes that X-ray attenuation arises as a composite effect of three substances

present within the scanned volume. Consequently, collagen concentration can be estimated as if collagen were the sole substance within the scanned volume. Collagen maps allow noninvasive quantification of collagen density and provide insights into altered biomechanical properties of the affected ligaments, facilitating a more precise anatomical–functional characterization of changes associated with inflammatory conditions.⁵³ Of note, initial studies suggest that, in CPPD, there is remodeling of the intrinsic and extrinsic ligament apparatus of the carpus, which is detectable using DECT-based collagen mapping.³⁶

Recent studies have shown that CT can provide insights into the mineralization of cartilage, which is particularly relevant in the context of osteoarthritis. Specifically, CT-measured mineralization of cartilage has been found to correlate with cartilage loss, indicating that alterations in mineral density may serve as a valuable biomarker for disease progression.^{54,55}

Periosteal proliferation

Periosteal proliferation, also known as protuberances, is a significant imaging finding typically observed in psoriatic arthritis, which is a crucial differential diagnosis of RA.⁵⁶ Unlike RA, psoriatic arthritis is an enthesitis-associated form of arthritis and is characterized by inflammatory changes affecting the attachments of tendons, ligaments, and joint capsules.⁵⁷ The protuberances often present as sharp extensions of cortical bone with a fuzzy, cloudy character and are located at the metaphyses of the phalanges, nail processes, and bony prominences such as the styloid process. In conjunction with erosive changes at the tendon insertions, characteristic signs are detectable by imaging, such as the “morning star” at the nail process or the “mouse ears” of the distal interphalangeal joints. In early disease, clearcut differentiation of such protuberances from degenerative osteophytic formations or erosions typically associated with RA may not always be possible by conventional X-ray. Conversely, CT imaging allows reliable differentiation of these distinct entities and also has a role in monitoring treatment responses.

Detection of active inflammation in joints and tendons

Active joint or tendon inflammation and its reliable detection are paramount in the initial diagnosis

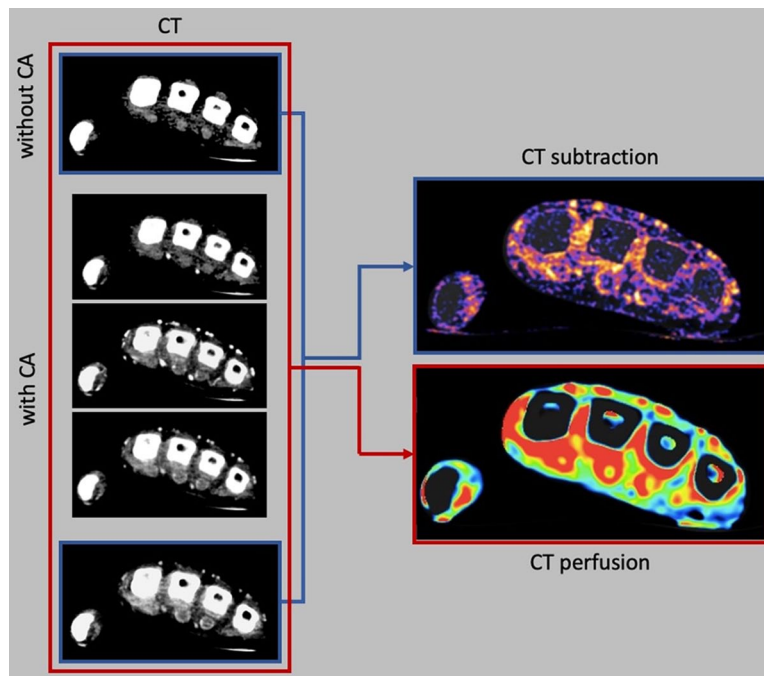


Figure 2. Reconstruction of CT subtraction and CT perfusion in a patient with severe synovitis of the metacarpophalangeal joints and severe tenosynovitis. CA, contrast agent; CT, computed tomography.

of arthritis for prompt initiation of appropriate therapy and justifying the use of sometimes costly treatments.⁵⁸ In clinical practice, ultrasound has established itself for identifying joint inflammation without administration of contrast agents by the presence of synovial thickening and increased Doppler signals.^{12,59} However, ultrasound crucially relies on the examiner's experience and cannot easily be standardized. For this reason, ultrasound is not recommended for serial monitoring of treatment and disease progression.⁶⁰

Conversely, MRI examinations can be excellently standardized. Its good soft tissue contrast and sensitivity to inflammatory changes after contrast agent administration make it an excellent tool for diagnosing active inflammation. However, a crucial drawback of MRI is its low specificity in identifying active inflammation. Therefore, current guidelines explicitly discourage the use of MRI as the primary imaging modality in early arthritis, reserving it for more complex and inconclusive cases.⁵⁹

Inflammatory joint/tendon lesions are characterized by higher contrast agent uptake compared with surrounding tissue on contrast-enhanced CT. Especially in anatomically complex regions

such as the hand, however, this specific contrast agent behavior often cannot be reliably identified without the use of suitable measurement methods due to image noise and intra- and interindividual variations in soft tissue density. As a result, CT has a somewhat secondary role in diagnosing active joint and tendon inflammation in clinical practice. Nevertheless, state-of-the-art technology and various reconstruction algorithms now allow the detection of active inflammation (see also Figure 2).

CT subtraction

CT subtraction can significantly improve the conspicuity of enhancing structures.^{15,16} Subtraction imaging was initially investigated using conventional CT, and promising results were achieved.¹⁶ In this approach, a CT scan is acquired before and after intravenous contrast agent administration. Subsequently, the unenhanced scan is subtracted from the contrast-enhanced scan, resulting in an image showing only the contrast agent. Subtraction imaging enables not only the detection of joint inflammation (synovitis) but also the assessment of inflammation along tendons (tenosynovitis/peritendinitis) and within bones. Initial pilot studies have

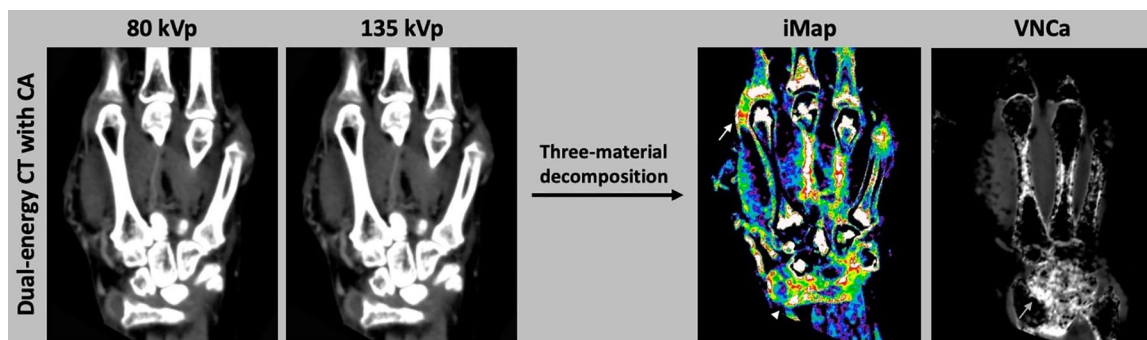


Figure 3. Dual-energy CT-based three-material decomposition to generate iMap and VNCa. iMap clearly shows severe synovitis of the second metacarpophalangeal joint (white arrow) and the wrist (white arrowhead). VNCa reveals higher water content in the wrist as a sign of bone marrow edema (gray arrow). CA, contrast agent; CT, computed tomography; iMap, iodine maps; VNCa, virtual non-calcium images.

demonstrated a sufficiently high sensitivity and specificity in the assessment of synovitis and tenosynovitis compared with MRI and ultrasound.¹⁵ Because two scans (before and after contrast agent administration) are acquired, patient compliance is of particular importance, as the reconstructed subtraction datasets are susceptible to motion artifacts.

CT perfusion

In addition to qualitative assessment of joint inflammation, CT also allows quantification of inflammatory activity. For this purpose, dynamic contrast-enhanced CT scans can be continuously acquired over a specific period of time for measurement of contrast enhancement in the synovium over time.^{61,62} The datasets can be used for the calculation of perfusion parameters in selected joints and tendons using region of interest (ROI) analysis.⁶³ This approach facilitates quantitative assessment of the severity of inflammatory activity, providing valuable insights, for example, into treatment responses. Dynamic contrast-enhanced CT or MRI is predominantly used in research settings, particularly for quantitative assessment of therapeutic responses in medication studies. Furthermore, dedicated acquisition protocols and postprocessing software are needed. This technical complexity has so far prevented the integration of dynamic contrast-enhanced CT or MRI into clinical practice.

Virtual monochromatic images

DECT allows the extraction of more in-depth information from the acquired image dataset than

conventional CT alone.⁶⁴ A case in point is the use of virtual monochromatic images (VMIs), which confer numerous advantages such as enhancing the visualization of iodine contrast and minimizing artifacts from metal implants. Low-energy VMIs imitate low photon energy without the drawbacks of a broad X-ray spectrum, resulting in better contrast between structures with different effective atomic numbers (Z_{eff}), such as iodinated contrast agents and soft tissues. The most significant enhancement of iodine contrast occurs at energy levels close to the k -edge of iodine, between 40 and 60 keV, albeit at the expense of increased image noise.⁶⁵ It has been demonstrated that, while VMIs detect inflammation with sufficient diagnostic accuracy, the improved contrast is offset by higher noise levels, rendering no discernible advantage for either quantitative or subjective evaluation.⁶⁶

Iodine maps for synovitis and tenosynovitis

Another method that has been proposed to improve the visualization of active inflammation is the computation of iodine maps using three-material decomposition.^{15,17} This DECT-specific reconstruction method provides additional information for the assessment and detection of inflammatory changes. It applies a three-material decomposition algorithm to the DECT dataset assuming that X-ray attenuation is determined by the sum of three substances present in the imaging volume. In this model, the concentration of the contrast agent (iodine) can be estimated, and virtual iodine maps can be computed to display the distribution and concentration of contrast (see Figure 3). The iodine maps facilitate the

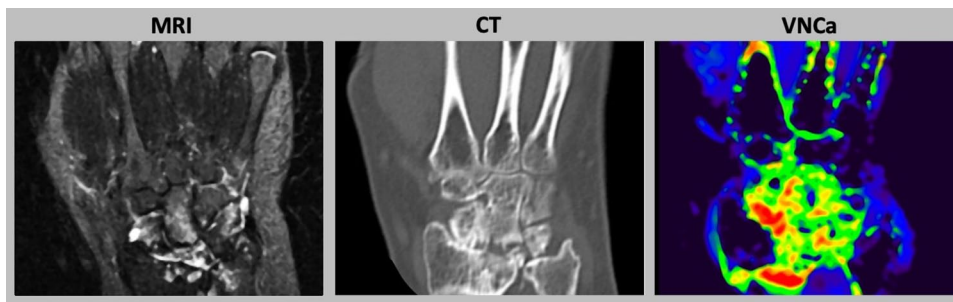


Figure 4. Bone marrow edema in a patient with severe rheumatoid arthritis. Bone marrow edema in the carpus is clearly visible in MRI and in dual-energy CT-based VNCa. Bone marrow edema is not visible in conventional CT.

CT, computed tomography; MRI, magnetic resonance imaging; VNCa, virtual non-calcium image.

assessment of contrast enhancement and enable quantitative measurement of iodine concentration.¹⁸ Consequently, valuable additional information regarding organ perfusion is obtained, which is also helpful in assessing treatment responses. However, inherent features of the reconstruction process result in lower sensitivity to contrast agent uptake compared with subtraction and pose disadvantages when other substances with relatively high atomic numbers (e.g., calcium in bones) coexist in an organ.¹⁵ On the other hand, the method is robust against motion artifacts and requires no precontrast scan. Iodine maps also facilitate the quantification of iodine content through ROI analysis, as suggested by initial pilot studies conducted in psoriatic arthritis and ongoing investigations.¹⁸

Virtual non-calcium images for osteitis

Osteitis, an inflammation of the bone, occurs in rheumatic diseases with severe inflammation or points to a differential diagnosis (e.g., psoriatic arthritis). It is a crucial prognostic indicator of impending joint destruction, requiring prompt therapeutic management. The bone marrow changes in osteitis are typically only detectable by MRI while both arthrosonography and conventional CT are clearly limited. However, initial studies have shown promising results with DECT.⁶⁷ Three-material differentiation allows specific depiction and quantification of calcium, quite similar to the iodine maps mentioned above.⁶⁸ Removing calcified bone by subtracting the calcium map from the original image improves the assessment of bone marrow. A higher proportion of water in the otherwise fatty bone marrow

in the subtraction image indicates the presence of bone marrow edema, for example, due to inflammation or trauma⁶⁹ (see Figures 3 and 4). Moreover, initial studies indicate that the use of iterative reconstruction can improve the visualization of bone marrow edema.⁷⁰

Advantages over MRI—imaging pitfalls

CT has several advantages over MRI. It is more widely available, and the examination generally takes less time than an MRI study. Despite radiation exposure and the administration of a contrast agent, patients also prefer CT over MRI, mostly because it is more comfortable.¹⁶ In the evaluation of structural changes, the much better spatial resolution of CT can counter the advantage of better soft tissue discrimination in MRI. Specifically, CT is better suited for differential diagnosis as it provides information beyond the detection of active inflammation and its distribution by allowing the identification of mild structural changes such as periosteal proliferation or small osteophytes and the detection of crystal disease (see Figure 5). This makes CT a very promising modality in arthritis imaging. For example, gouty tophi are difficult to detect by MRI and usually require an additional ultrasound or X-ray examination. Furthermore, DECT allows robust differentiation of the various crystal arthropathies based on their tissue properties, which is essential for initiating appropriate therapeutic management and prevention of irreversible joint damage.

For certain clinical questions, direct intra-articular contrast administration in CT can be helpful, for instance, when assessing ligamentous structures.⁷²

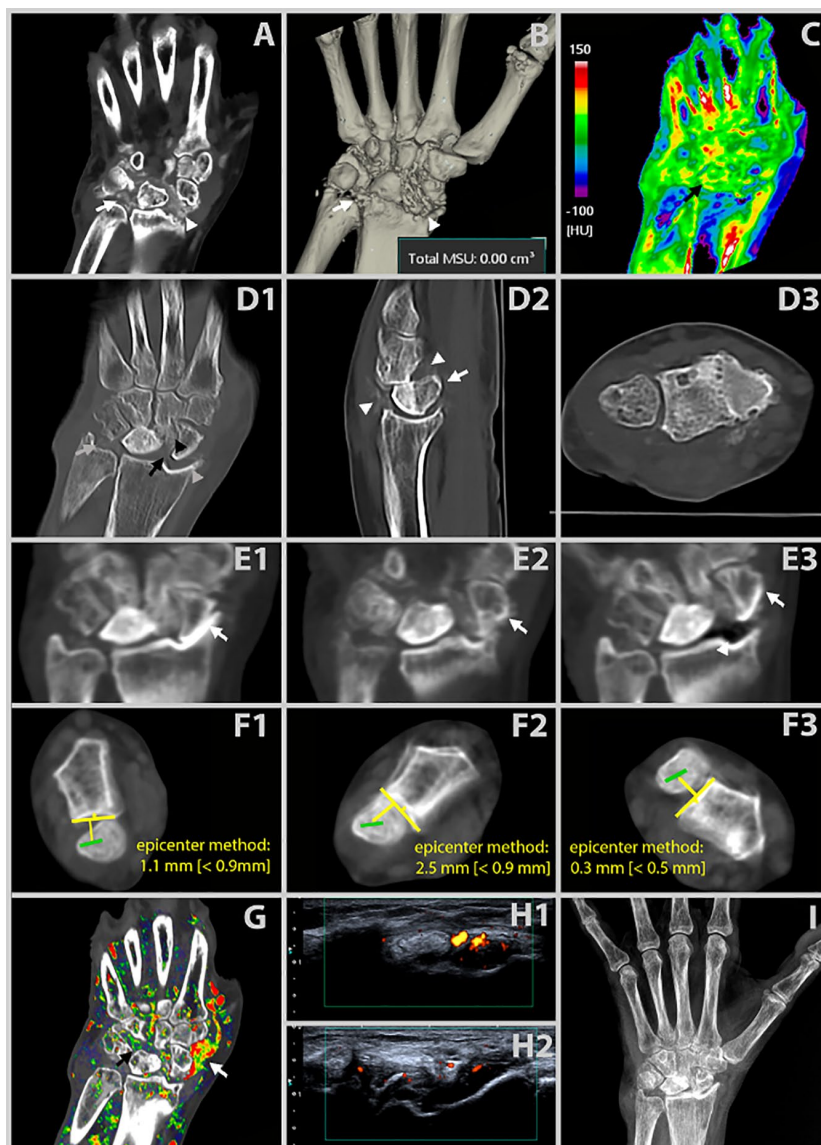


Figure 5. Imaging examples of a 73-year-old patient with clinical suspicion of rheumatoid arthritis. CT revealed the diagnosis of CPPD arthropathy. (a) CPPD-typical calcifications of the SL ligament (white arrowhead) and of the TFCC and lunotriquetral ligament (white arrow) are clearly visible. (b) In the corresponding uric acid reconstruction, the calcifications show no uric acid content (white arrow and white arrowhead), thus ruling out gouty arthritis. (c) VNCa shows bone marrow edema/necrosis of the lunate (black arrow). (d1) Static CT shows a dissociation of the SL joint space (black arrow) with accompanying radiocarpal joint osteoarthritis (gray arrowhead), indicative of static SL ligament instability. In addition, there is a narrowing of the capitulum joint space visible, along with the beginning of proximal migration of the capitate (black arrowhead). (d2) In the sagittal plane, subluxation of the lunate is recognizable (white arrow). (d3) In the axial plane, the position of the DRUJ is normal. (e) 4D-CT in ulnar abduction reveals increasing migration of the scaphoid bone during ulnar abduction (white arrow) with a vacuum phenomenon (white arrowhead). (f) 4D-CT in rotation shows subluxation of the DRUJ in supination using the epicenter method.⁷¹ Green line: the line between the center of the styloid process to the center of the ulna to determine the center of rotation of the DRUJ. It is crucial that the line perpendicular to the chord of the sigmoid notch points to the middle half of the sigmoid notch (yellow line). In this example, a deviation of up to 2.5 mm from this point is observed, indicating DRUJ instability. (g) CT subtraction with severe synovitis in the radial carpus (white arrow) and the intercarpal joint (black arrow). (h1) Sonography of the wrist in the transversal plane with tenosynovitis. (h2) Sonography of the wrist in the longitudinal plane showing effusion and crystals in the wrist. (i) X-ray shows crystals in the carpus and static SL instability.
CPPD, calcium pyrophosphate deposition; CT, computed tomography; 4D-CT, four-dimensional computed tomography; DRUJ, distal radioulnar joint; SL, scapholunate; TFCC, triangular fibrocartilage complex; VNCa, virtual non-calcium image.

However, it is important to note that this is an invasive procedure with a high risk of complications, such as joint infection. In addition, this technique requires significant technical resources and trained personnel, which significantly influences its use in routine clinical practice. Moreover, initial studies showed potential chondrotoxicity of certain local anesthetics, raising concerns about the use of intra-articular contrast agents.⁷³ These factors underscore the need for careful consideration of the utility of CT arthrography compared to other imaging modalities, particularly in patients with pre-existing chondral damage due to arthritis.

Outlook

The field of CT imaging has seen rapid advancements, leading to a deeper understanding of diseases and an expanded range of clinical applications. Since its introduction, CT technology has significantly improved in terms of speed, spatial resolution, and dose efficiency, leading to important clinical applications and a large impact on medical care. Important advances include 4D-CT and photon-counting CT (PCCT). PCCT has broad potential in clinical practice.⁷⁴ Unlike conventional CT, which is based on energy integration, PCCT counts individual photons, resulting in a more precise differentiation of energies. This, in turn, leads to improved contrast resolution with lower radiation exposure.⁷⁵ The ability to detect individual photons also opens up new possibilities for material differentiation and was shown to further improve soft tissue imaging, contrast agent identification,⁷⁶ and discrimination between various crystal arthropathies.^{77,78} Furthermore, the assessment of cartilage pathologies using advanced CT arthrography techniques is an evolving field of research, with initial experimental studies yielding promising results.^{79,80}

Conclusion

In this review, we explored the different applications of CT in arthritis imaging and their clinical relevance. In conjunction with different reconstruction algorithms, more information can be derived from CT and DECT images, making them a crucial tool in multiparametric imaging in arthritis. Ongoing technical advances not only promise higher diagnostic accuracy but also have the potential to significantly expand the applications of CT in the diagnosis of arthritis and patient management in the near future.

Declarations

Ethics approval and consent to participate

Not applicable.

Consent for publication

Not applicable.

Author contributions

Sevtap Tugce Ulas: Conceptualization; Investigation; Methodology; Project administration; Visualization; Writing – original draft; Writing – review & editing.

Torsten Diekhoff: Conceptualization; Formal analysis; Supervision; Validation; Visualization; Writing – original draft; Writing – review & editing.

Acknowledgements

The authors thank Ms Bettina Herwig for language editing and the Berlin Institute of Health for personal funding (S.T.U. and T.D.).

Funding

The authors received no financial support for the research, authorship, and/or publication of this article.

Competing interests

S.T.U. reports funding from the Berlin Institute of Health (BIH) during the conduct of this study (Junior Digital Clinician Scientist Program). T.D. reports personal fees from MSD, Novartis, and Eli Lilly outside the submitted work and reports funding from the BIH during the conduct of this study.

Availability of data and materials

Not applicable.

ORCID iD

Sevtap Tugce Ulas  <https://orcid.org/0000-0003-3871-3746>

References

1. Mallinson PI, Coupal TM, McLaughlin PD, et al. Dual-energy CT for the musculoskeletal system. *Radiology* 2016; 281: 690–707.
2. Bursill D, Taylor WJ, Terkeltaub R, et al. Gout, hyperuricaemia and crystal-associated disease network (G-CAN) consensus statement regarding

- labels and definitions of disease states of gout. *Ann Rheum Dis* 2019; 78: 1592–1600.
3. Kotlyarov M, Hermann KGA, Mews J, et al. Development and validation of a quantitative method for estimation of the urate burden in patients with gouty arthritis using dual-energy computed tomography. *Eur Radiol* 2020; 30: 404–412.
 4. Ramon A, Bohm-Sigraund A, Pottecher P, et al. Role of dual-energy CT in the diagnosis and follow-up of gout: systematic analysis of the literature. *Clin Rheumatol* 2018; 37: 587–595.
 5. Neogi T, Jansen TL, Dalbeth N, et al. 2015 Gout classification criteria: an American College of Rheumatology/European League Against Rheumatism collaborative initiative. *Ann Rheum Dis* 2015; 74: 1789–1798.
 6. Richette P, Doherty M, Pascual E, et al. 2018 updated European League Against Rheumatism evidence-based recommendations for the diagnosis of gout. *Ann Rheum Dis* 2020; 79: 31–38.
 7. Mandl P, D'Agostino MA, Navarro-Compan V, et al. 2023 EULAR recommendations on imaging in diagnosis and management of crystal-induced arthropathies in clinical practice. *Ann Rheum Dis* 2024; 83: 752–759.
 8. Knevel R, Lukas C, van der Heijde D, et al. Defining erosive disease typical of RA in the light of the ACR/EULAR 2010 criteria for rheumatoid arthritis; results of the data driven phase. *Ann Rheum Dis* 2013; 72: 590–595.
 9. Drosos AA, Pelechas E and Voulgari PV. Conventional radiography of the hands and wrists in rheumatoid arthritis. What a rheumatologist should know and how to interpret the radiological findings. *Rheumatol Int* 2019; 39: 1331–1341.
 10. Forghani R, De Man B and Gupta R. Dual-energy computed tomography: physical principles, approaches to scanning, usage, and implementation: part 1. *Neuroimaging Clin N Am* 2017; 27: 371–384.
 11. Johnson TR, Krauss B, Sedlmair M, et al. Material differentiation by dual energy CT: initial experience. *Eur Radiol* 2007; 17: 1510–1517.
 12. Colebatch AN, Edwards CJ, Ostergaard M, et al. EULAR recommendations for the use of imaging of the joints in the clinical management of rheumatoid arthritis. *Ann Rheum Dis* 2013; 72: 804–814.
 13. Ostergaard M and Boesen M. Imaging in rheumatoid arthritis: the role of magnetic resonance imaging and computed tomography. *Radiol Med* 2019; 124: 1128–1141.
 14. Fukuda T, Umezawa Y, Tojo S, et al. Initial experience of using dual-energy CT with an iodine overlay image for hand psoriatic arthritis: comparison study with contrast-enhanced MR imaging. *Radiology* 2017; 284: 134–142.
 15. Ulas ST, Ziegeler K, Richter ST, et al. Contrast-enhanced CT techniques and MRI perform equally well in arthritis imaging of the hand: a prospective diagnostic accuracy study. *Eur Radiol* 2022; 32(9): 6376–6383.
 16. Diekhoff T, Ulas ST, Poddubnyy D, et al. Ultra-low-dose CT detects synovitis in patients with suspected rheumatoid arthritis. *Ann Rheum Dis* 2019; 78: 31–35.
 17. Fukuda T, Umezawa Y, Asahina A, et al. Dual energy CT iodine map for delineating inflammation of inflammatory arthritis. *Eur Radiol* 2017; 27: 5034–5040.
 18. Kayama R, Fukuda T, Ogiwara S, et al. Quantitative analysis of therapeutic response in psoriatic arthritis of digital joints with dual-energy CT iodine maps. *Sci Rep* 2020; 10: 1225.
 19. Große Hokamp N, Laukamp KR, Lennartz S, et al. Artifact reduction from dental implants using virtual monoenergetic reconstructions from novel spectral detector CT. *Eur J Radiol* 2018; 104: 136–142.
 20. Gervaise A, Osemont B, Lecocq S, et al. CT image quality improvement using Adaptive Iterative Dose Reduction with wide-volume acquisition on 320-detector CT. *Eur Radiol* 2012; 22: 295–301.
 21. Vardhanabhuti V, Riordan RD, Mitchell GR, et al. Image comparative assessment using iterative reconstructions: clinical comparison of low-dose abdominal/pelvic computed tomography between adaptive statistical, model-based iterative reconstructions and traditional filtered back projection in 65 patients. *Invest Radiol* 2014; 49: 209–216.
 22. Brinkmann GH, Norli ES, Boyesen P, et al. Role of erosions typical of rheumatoid arthritis in the 2010 ACR/EULAR rheumatoid arthritis classification criteria: results from a very early arthritis cohort. *Ann Rheum Dis* 2017; 76: 1911–1914.
 23. Smolen JS, Aletaha D and McInnes IB. Rheumatoid arthritis. *Lancet* 2016; 388: 2023–2038.
 24. Lee CH, Srikkum W, Burghardt AJ, et al. Correlation of structural abnormalities of the wrist and metacarpophalangeal joints evaluated by high-resolution peripheral quantitative computed tomography, 3 Tesla magnetic

- resonance imaging and conventional radiographs in rheumatoid arthritis. *Int J Rheum Dis* 2015; 18: 628–639.
25. Perry D, Stewart N, Benton N, et al. Detection of erosions in the rheumatoid hand; a comparative study of multidetector computerized tomography versus magnetic resonance scanning. *J Rheumatol* 2005; 32: 256–267.
 26. Ulas ST, Ziegeler K, Richter ST, et al. CT-like images in MRI improve specificity of erosion detection in patients with hand arthritis: a diagnostic accuracy study with CT as standard of reference. *RMD Open* 2022; 8: e002089.
 27. Ulas ST, Diekhoff T, Hermann KGA, et al. Susceptibility-weighted MR imaging to improve the specificity of erosion detection: a prospective feasibility study in hand arthritis. *Skeletal Radiol* 2019; 48: 721–728.
 28. Schwaiger BJ, Schneider C, Kronthaler S, et al. CT-like images based on T1 spoiled gradient-echo and ultra-short echo time MRI sequences for the assessment of vertebral fractures and degenerative bone changes of the spine. *Eur Radiol* 2021; 31: 4680–4689.
 29. Breighner RE, Endo Y, Konin GP, et al. Technical developments: zero echo time imaging of the shoulder: enhanced osseous detail by using MR imaging. *Radiology* 2018; 286: 960–966.
 30. Florkow MC, Zijlstra F, Willemsen K, et al. Deep learning-based MR-to-CT synthesis: the influence of varying gradient echo-based MR images as input channels. *Magn Reson Med* 2020; 83: 1429–1441.
 31. Rauch A, Arab WA, Dap F, et al. Four-dimensional CT analysis of wrist kinematics during radioulnar deviation. *Radiology* 2018; 289: 750–758.
 32. Zhao K, Breighner R, Holmes D 3rd, et al. A technique for quantifying wrist motion using four-dimensional computed tomography: approach and validation. *J Biomech Eng* 2015; 137: 0745011–0745015.
 33. Leng S, Zhao K, Qu M, et al. Dynamic CT technique for assessment of wrist joint instabilities. *Med Phys* 2011; 38(Suppl. 1): S50.
 34. Gondim Teixeira PA, Formery AS, Hossu G, et al. Evidence-based recommendations for musculoskeletal kinematic 4D-CT studies using wide area-detector scanners: a phantom study with cadaveric correlation. *Eur Radiol* 2017; 27: 437–446.
 35. Ulas ST, Pochandke L, Ohrndorf S, et al. Four-dimensional computed tomography detects dynamic three-dimensional pathologies of the wrist in patients with calcium pyrophosphate deposition disease. *Front Med* 2023; 10: 1231667.
 36. Ziegeler K, Richter ST, Hermann S, et al. Dual-energy CT collagen density mapping of wrist ligaments reveals tissue remodeling in CPPD patients: first results from a clinical cohort. *Skeletal Radiol* 2021; 50: 417–423.
 37. Diekhoff T, Kiefer T, Stroux A, et al. Detection and characterization of crystal suspensions using single-source dual-energy computed tomography: a phantom model of crystal arthropathies. *Invest Radiol* 2015; 50: 255–260.
 38. Martinon F, Petrilli V, Mayor A, et al. Gout-associated uric acid crystals activate the NALP3 inflammasome. *Nature* 2006; 440: 237–241.
 39. Ziegeler K, Diekhoff T, Hermann S, et al. Low-dose computed tomography as diagnostic tool in calcium pyrophosphate deposition disease arthropathy: focus on ligamentous calcifications of the wrist. *Clin Exp Rheumatol* 2019; 37: 826–833.
 40. Ziegeler K, Hermann S, Hermann KGA, et al. Dual-energy CT in the differentiation of crystal depositions of the wrist: does it have added value? *Skeletal Radiol* 2020; 49: 707–713.
 41. Abhishek A, Tedeschi SK, Pascart T, et al. The 2023 ACR/EULAR classification criteria for calcium pyrophosphate deposition disease. *Ann Rheum Dis* 2023; 82: 1248–1257.
 42. Pascart T, Norberciak L, Legrand J, et al. Dual-energy computed tomography in calcium pyrophosphate deposition: initial clinical experience. *Osteoarthritis Cartilage* 2019; 27: 1309–1314.
 43. Pascart T, Falgayrac G, Norberciak L, et al. Dual-energy computed-tomography-based discrimination between basic calcium phosphate and calcium pyrophosphate crystal deposition in vivo. *Ther Adv Musculoskelet Dis* 2020; 12: 1759720X20936060.
 44. Tedeschi SK, Solomon DH, Yoshida K, et al. A prospective study of dual-energy CT scanning, US and X-ray in acute calcium pyrophosphate crystal arthritis. *Rheumatology (Oxford)* 2020; 59: 900–903.
 45. Budzik JF, Marzin C, Legrand J, et al. Can dual-energy computed tomography be used to identify early calcium crystal deposition in the knees of patients with calcium pyrophosphate deposition? *Arthritis Rheumatol* 2021; 73: 687–692.
 46. Jarraya M, Bitoun O, Wu D, et al. Dual energy computed tomography cannot effectively differentiate between calcium pyrophosphate and

- basic calcium phosphate diseases in the clinical setting. *Osteoarthr Cartil Open* 2024; 6: 100436.
47. Bongartz T, Glazebrook KN, Kavros SJ, et al. Dual-energy CT for the diagnosis of gout: an accuracy and diagnostic yield study. *Ann Rheum Dis* 2015; 74: 1072–1077.
 48. Choi HK, Al-Arfaj AM, Eftekhari A, et al. Dual energy computed tomography in tophaceous gout. *Ann Rheum Dis* 2009; 68: 1609–1612.
 49. Ottaviani S. Imaging follow-up of MSU crystal depletion. *Gout Urate Cryst Depos Dis* 2024; 2: 34–44.
 50. Klauser AS, Halpern EJ, Strobl S, et al. Dual-energy computed tomography detection of cardiovascular monosodium urate deposits in patients with gout. *JAMA Cardiol* 2019; 4: 1019–1028.
 51. Pascart T, Carpentier P, Choi HK, et al. Identification and characterization of peripheral vascular color-coded DECT lesions in gout and non-gout patients: The VASCURATE study. *Semin Arthritis Rheum* 2021; 51: 895–902.
 52. Pascart T and Budzik J-F. Does monosodium urate crystal vascular deposition exist? Review of the evidence. *Gout Urate Cryst Depos Dis* 2023; 1: 208–216.
 53. Wittig TM, Ziegeler K, Kreutzinger V, et al. Dual-energy computed tomography collagen density mapping of the cranio-cervical ligaments—a retrospective feasibility study. *Diagnostics (Basel)* 2022; 12: 2966.
 54. Legrand J, Marzin C, Neogi T, et al. Associations of changes in knee hyaline cartilage composition measured with dual-energy computed tomography in gout, aging and osteoarthritis. *Cartilage* 2024; 15: 283–292.
 55. Liew JW, Jarraya M, Guermazi A, et al. Intra-articular mineralization on computerized tomography of the knee and risk of cartilage damage: the multicenter osteoarthritis study. *Arthritis Rheumatol* 2024; 76: 1054–1061.
 56. Narvaez J, Narvaez JA, de Albert M, et al. Can magnetic resonance imaging of the hand and wrist differentiate between rheumatoid arthritis and psoriatic arthritis in the early stages of the disease? *Semin Arthritis Rheum* 2012; 42: 234–245.
 57. Ostergaard M and Maksymowych WP. Advances in the evaluation of peripheral enthesitis by magnetic resonance imaging in patients with psoriatic arthritis. *J Rheumatol* 2023; 50: 18–22.
 58. Scott DL, Wolfe F and Huizinga TW. Rheumatoid arthritis. *Lancet* 2010; 376: 1094–1108.
 59. Combe B, Landewe R, Daien CI, et al. 2016 Update of the EULAR recommendations for the management of early arthritis. *Ann Rheum Dis* 2017; 76: 948–959.
 60. Smolen JS, Landewe RBM, Bijlsma JWJ, et al. EULAR recommendations for the management of rheumatoid arthritis with synthetic and biological disease-modifying antirheumatic drugs: 2019 update. *Ann Rheum Dis* 2020; 79: 685–699.
 61. Axelsen MB, Poggenborg RP, Stoltenberg M, et al. Reliability and responsiveness of dynamic contrast-enhanced magnetic resonance imaging in rheumatoid arthritis. *Scand J Rheumatol* 2013; 42: 115–122.
 62. Wojciechowski W, Tabor Z and Urbanik A. Assessing synovitis based on dynamic gadolinium-enhanced MRI and EULAR-OMERACT scores of the wrist in patients with rheumatoid arthritis. *Clin Exp Rheumatol* 2013; 31: 850–856.
 63. Ulas ST, Hermann KG, Makowski MR, et al. Perfusion in hand arthritis on dynamic contrast-enhanced computed tomography: a randomized prospective study using MRI as a standard of reference. *Skeletal Radiol* 2021; 50: 59–68.
 64. Goo HW and Goo JM. Dual-energy CT: new horizon in medical imaging. *Korean J Radiol* 2017; 18: 555–569.
 65. Leng S, Yu L, Fletcher JG, et al. Maximizing iodine contrast-to-noise ratios in abdominal CT imaging through use of energy domain noise reduction and virtual monoenergetic dual-energy CT. *Radiology* 2015; 276: 562–570.
 66. Ulas ST, Ziegeler K, Richter ST, et al. Virtual monochromatic images from dual-energy computed tomography do not improve the detection of synovitis in hand arthritis. *Diagnostics (Basel)* 2022; 12: 1891.
 67. Diekhoff T, Scheel M, Hermann S, et al. Osteitis: a retrospective feasibility study comparing single-source dual-energy CT to MRI in selected patients with suspected acute gout. *Skeletal Radiol* 2017; 46: 185–190.
 68. Jans L, De Kock I, Herregods N, et al. Dual-energy CT: a new imaging modality for bone marrow oedema in rheumatoid arthritis. *Ann Rheum Dis* 2018; 77: 958–960.
 69. Ghazi Sherbaf F, Sair HI, Shakoor D, et al. DECT in detection of vertebral fracture-associated bone marrow edema: a systematic review and meta-analysis with emphasis on technical and imaging interpretation parameters. *Radiology* 2021; 300: 110–119.

70. Engelhard N, Hermann KG, Greese J, et al. Single-source dual-energy computed tomography for the detection of bone marrow lesions: impact of iterative reconstruction and algorithms. *Skeletal Radiol* 2020; 49: 765–772.
71. Wechsler RJ, Wehbe MA, Rifkin MD, et al. Computed tomography diagnosis of distal radioulnar subluxation. *Skeletal Radiol* 1987; 16: 1–5.
72. Hesse N, Schmitt R, Luitjens J, et al. Carpal instability: II. Imaging. *Semin Musculoskelet Radiol* 2021; 25: 304–310.
73. Parker EB, Hering KA, Chiodo CP, et al. Intraarticular injections in the foot and ankle: medication selection patterns and perceived risk of chondrotoxicity. *Foot Ankle Orthop* 2023; 8: 24730114231216990.
74. Nakamura Y, Higaki T, Kondo S, et al. An introduction to photon-counting detector CT (PCD CT) for radiologists. *Jpn J Radiol* 2023; 41: 266–282.
75. Anhaus JA, Heider M, Killermann P, et al. A new iterative metal artifact reduction algorithm for both energy-integrating and photon-counting CT systems. *Invest Radiol* 2024; 59: 526–537.
76. Mese I, Altintas Taslicay C and Sivrioglu AK. Synergizing photon-counting CT with deep learning: potential enhancements in medical imaging. *Acta Radiol* 2024; 65(2):159–166.
77. Stamp LK, Anderson NG, Becce F, et al. Clinical utility of multi-energy spectral photon-counting computed tomography in crystal arthritis. *Arthritis Rheumatol* 2019; 71: 1158–1162.
78. Mourad C, Gallego Manzano L, Viry A, et al. Chances and challenges of photon-counting CT in musculoskeletal imaging. *Skeletal Radiol* 2024; 53: 1889–1902.
79. Rajendran K, Murthy NS, Frick MA, et al. Quantitative knee arthrography in a large animal model of osteoarthritis using photon-counting detector CT. *Invest Radiol* 2020; 55: 349–356.
80. Hall ME, Wang AS, Gold GE, et al. Contrast solution properties and scan parameters influence the apparent diffusivity of computed tomography contrast agents in articular cartilage. *J R Soc Interface* 2022; 19: 20220403.

Visit Sage journals online
journals.sagepub.com/
home/tab

 Sage journals